Dept. of Math. University of Oslo
Pure Mathematics No. 36
ISSN 0806–2439 November 2005

ROBUST CONVERGENCE OF MULTI POINT FLUX APPROXIMATION ON ROUGH GRIDS

RUNHILD A. KLAUSEN* AND RAGNAR WINTHER†

Abstract.
This paper establishes the convergence of a multi point flux approximation control volume method on rough quadrilateral grids. By rough grids we refer to a family of refined quadrilateral grids where the cells are not required to approach parallelograms in the asymptotic limit. In contrast to previous convergence results for these methods we consider here a version where the flux approximation is derived directly in the physical space, and not on a reference cell. As a consequence, less regular grids are allowed. However, the extra cost is that the symmetry of the method is lost.

1. Introduction. The multi point flux approximation (MPFA) is a control volume method developed by the oil industry as a reliable discretization of the pressure equation, derived from Darcy's law, on general rough quadrilateral and hexahedral grids. In reservoir simulation the geology of the reservoir, which includes faults and non parallel layers in the media, is a major challenge. The MPFA method provides a local explicit flux with respect to the pressure. This is the main advantage compared to the mixed finite element method, and allows a wider class of applications. For example, when the pressure equation occurs as a subsystem of a multi phase model, a fully implicit discretization of the system becomes possible with acceptable cost. There is by now a number of papers on the MPFA approach, cf. for example the overview papers [1, 13, 15, 16].

So far the theoretical convergence properties of MPFA methods are not well enough understood. In [17] we analyze an MPFA method which is derived from a mapping onto an orthogonal reference cell. The analysis is based on an equivalence to a mixed finite element method with a broken Raviart-Thomas space and a specific quadrature rule. However, the analysis requires so called h^2*–uniform* grids, i.e. the cells are required to approach parallelograms as the grid is refined. An alternative analysis of essentially the same method, with the same grid restriction, is done in [19] using a relation to the lowest order Brezzi-Douglas-Marini element instead. In fact, it is shown numerically in [4] that "the reference space MPFA method" diverges on irregular grids.

The lack of grid robustness for the reference space MPFA corresponds to an analog property for the standard mixed finite element method, when the finite element spaces are derived from a bilinear mapping of a unit square. In a series of papers [6, 7, 8], Arnold, Boffi, and Falk discuss this and show divergence in the standard norms for elements like the Raviart–Thomas and the Brezzi–Douglas–Marini elements on rough grids. The essential cause of the problem is the fact that Jacobian matrix of the bilinear map is only constant when the grid cells are parallelograms. To overcome the defect, and to obtain mixed methods which converge on rough grids, they propose to modify the finite element spaces.

Based on numerical experiments it is shown in [3, 4, 14], that a corresponding grid robustness of the MPFA method is obtained if the flux approximation is derived directly in the physicals space. The purpose of the present paper is to give a theoretical justification for this experimental fact. We will indeed show that the physical

*Centre of Mathematics for Applications, University of Oslo, and Centre for Integrated Petroleum Research, University of Bergen. P.O. Box 1053 Blindern, 0316 Oslo 3, Norway (runhildk@ifi.uio.no).
†Centre of Mathematics for Applications and Departement of Informatics, University of Oslo. P.O. Box 1053 Blindern, 0316 Oslo 3, Norway (rwinther@cma.uio.no).

space derived MPFA method presented below converges on rough grids. The method analyzed here has the property that it is locally exact on uniform flow, a property not shared by the method studied in [17]. However, the prize to pay for this robustness is a non symmetric coefficient operator, and as a consequence, a weaker, but non asymptotic shape condition is required to obtain stability of the method.

In this paper the analysis is restricted to two space dimensions. Let Ω be a bounded domain in $\boldsymbol{R}^2$, with polygonal boundary $\partial\Omega$. The problem discussed in this paper is the elliptic equation,

$$-\mathrm{div}\,(\boldsymbol{K}(\boldsymbol{x})\mathrm{grad}\,p) = g \text{ in } \Omega, \tag{1.1}$$

$$p(\boldsymbol{x}) = 0 \text{ on } \partial\Omega.$$

This is to be viewed as a prototype for the pressure equation in porous medium flow, where $\boldsymbol{K}$ the permeability, and $\boldsymbol{u} = -\boldsymbol{K}\,\mathrm{grad}\,p$ the Darcy velocity. The boundary condition is chosen for simplicity of exposition.

As is more or less standard for control volume methods, cf. for example [5, 9, 11], the analysis below will be done by identifying an equivalence between the physical space MPFA method and a proper mixed finite element method, using a specific numerical integration rule and broken Raviart–Thomas space. In fact, the proper mixed finite element method and the numerical quadrature rule are derived in Sections 2 and 3, independently of any relation to an MPFA method. The main error estimates for this mixed method are established in Section 4. In Section 5 we present numerical results which shows the advantage of the method discussed here compared to the reference space derived method analyzed in [17]. Then, finally in an Appendix our mixed finite element method is shown to be equivalent to the physical space derived MPFA method proposed originally in [2].

2. Preliminaries. Let $\mathcal{L}_2(E)$ denote the square Lebesgue-integrable function on the domain $E \subset \boldsymbol{R}^2$ with inner-product $(\cdot\,,\cdot)_E$ and norm $\|\cdot\|_E = (\cdot\,,\cdot)_E^{1/2}$. If E equals the domain Ω of (1.1) introduced above the subscript will be dropped. Also, let $H^1(E)$ denote the Sobolev space of first order differentiable functions in $\mathcal{L}_2(E)$, with norm

$$\|q\|_{1,E} = (\|q\|_E^2 + |q|_{1,E}^2)^{1/2},$$

and with the associated seminorm

$$|q|_{1,E} = \|\,\mathrm{grad}\,q\|_E.$$

The space

$$H(\mathrm{div}; E) = \{\boldsymbol{v} \in (\mathcal{L}_2(E))^2 : \mathrm{div}\,\boldsymbol{v} \in \mathcal{L}_2(E)\},$$

is equipped with the norm

$$\|\boldsymbol{v}\|_{\mathrm{div},E} = (\|\boldsymbol{v}\|_E^2 + \|\,\mathrm{div}(\boldsymbol{v})\|_E^2)^{1/2}.$$

Also, let P_k be the set of polynomials of degree k. The permeability $\boldsymbol{K}$ is a symmetric tensor which is uniformly positive definite in Ω. In fact, it is an important feature of reservoir simulation that $\boldsymbol{K}$ is allowed to be discontinuous, and both the MPFA method and the mixed finite element method adapt to this case. However, for the convergence analysis presented in this paper we need the components of $\boldsymbol{K}$ to be

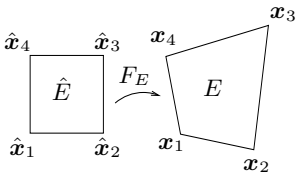

FIG. 2.1. *mapping F_E from $\hat{E}$ into E.*

$C^1(\bar{\Omega})$, and the Darcy velocity is assumed to satisfy $\boldsymbol{u} \in (H^1(\Omega))^2$. This regularity is for example ensured if the domain Ω is convex, and $g \in \mathcal{L}_2$. In special cases discontinuous coefficients still give some smoothness of the solution, and for such cases relaxed smoothness condition on the permeability is allowed.

Let $\{\mathcal{T}_h\}$ denote a family of partitions of Ω into quadrilateral subdomains, or cells, where h is the maximum element edge. We will assume that the family is regular, cf. [12, page 246–247], i.e. all cells are convex, the angles are uniformly bounded away from zero and π, and the ratio between the length of the smallest edge and the diameter of the cell is uniformly bounded from below. Assume further that each interior vertex of $\mathcal{T}_h$ meets four cells. Finally, denote the set of edges of $\mathcal{T}_h$ by $\mathcal{E}_h$.

In order to define the proper finite element method below we need to introduce certain finite dimensional function spaces. In particular, we shall introduce a subspace of $H(\mathrm{div})$ which can be referred to as a splitting of the lowest order Raviart-Thomas space over a quadrilateral.

2.1. Quadrilaterals. For any quadrilateral subdomain we will utilize a bilinear mapping $F = F_E : \hat{E} \to E$ which is smooth and invertible, see Figure 2.1. The reference space $\hat{E} = (0,1) \times (0,1)$ is the unit square. Let $\boldsymbol{x}_i = (x_i, y_i)$, $i = 1, 2, 3, 4$, be the four vertices of E in counterclockwise direction as shown in Figure 2.1. If $\boldsymbol{x}_{ij} = (\boldsymbol{x}_i - \boldsymbol{x}_j)$ the transformation F takes the form

$$F(\hat{x}, \hat{y}) = \boldsymbol{x}_1 + \boldsymbol{x}_{21}\hat{x} + \boldsymbol{x}_{41}\hat{y} + (\boldsymbol{x}_{32} - \boldsymbol{x}_{41})\hat{x}\hat{y} \tag{2.1}$$

for $(\hat{x}, \hat{y}) \in \hat{E}$. The Jacobian matrix of F is denoted $\boldsymbol{D} = \boldsymbol{D}_E$ and $J = J_E$ the Jacobian of the mapping.

A orthogonal reference space is a basic assumption in the construction of Raviart-Thomas elements on quadrilateral grids. As will be shown, we relate the mixed finite element method based on such a reference mapping onto a square reference space, to MPFA derived without this mapping.

If $\hat{\boldsymbol{v}}$ is a vector field in $H(\mathrm{div}, \hat{E})$, define a vector field $\boldsymbol{v}$ on E by the Piola transform $\mathcal{P} = \mathcal{P}_E$, i.e.

$$\boldsymbol{v}(\boldsymbol{x}) = \mathcal{P}\hat{\boldsymbol{v}}(\boldsymbol{x}) = \frac{1}{J}\boldsymbol{D}\hat{\boldsymbol{v}} \circ F^{-1}(\boldsymbol{x}).$$

Then $\int_E \mathrm{div}\, \boldsymbol{v}\, q\, d\boldsymbol{x} = \int_{\hat{E}} \mathrm{div}\, \hat{\boldsymbol{v}}\, \hat{q}\, d\hat{\boldsymbol{x}}$ for all $q \in \mathcal{L}_2$ when $\hat{q} = q \circ F$. Therefore,

$$\mathrm{div}\, \hat{\boldsymbol{v}} = J\, \mathrm{div}\, \boldsymbol{v} \tag{2.2}$$

and

$$\int_e \boldsymbol{v} \cdot \boldsymbol{n}\, ds = \int_{\hat{e}} \hat{\boldsymbol{v}} \cdot \hat{\boldsymbol{n}}\, d\hat{s},$$

where s and $\hat{s}$ denote the arc length along the edges e and $\hat{e}$, respectively, with $\boldsymbol{n}$ and $\hat{\boldsymbol{n}}$ as the unit normal vectors, cf. [10].

Define the analog reference permeability as $\hat{\boldsymbol{K}} = \mathrm{J}\boldsymbol{D}^{-1}\boldsymbol{K}\boldsymbol{D}^{-T}$. Note that $\hat{\boldsymbol{K}}$ is symmetric positive definite and bounded from above and below independent of h. Now

$$\hat{\boldsymbol{K}}^{-1} = J^{-1}\boldsymbol{D}^T\boldsymbol{K}^{-1}\boldsymbol{D}$$

and

$$(\boldsymbol{K}^{-1}\boldsymbol{u}, \boldsymbol{v})_E = (J\,\boldsymbol{K}^{-1}\,\frac{1}{J}\boldsymbol{D}\hat{\boldsymbol{u}}, \frac{1}{J}\boldsymbol{D}\hat{\boldsymbol{v}})_{\hat{E}} = (\hat{\boldsymbol{K}}^{-1}\hat{\boldsymbol{u}}, \hat{\boldsymbol{v}})_{\hat{E}}.$$

The matrix field $\hat{\boldsymbol{K}}$ embodies both the permeability and the shape of the cells, and will be an essential factor in the further discussions and results. If $\hat{\boldsymbol{K}}$ is diagonal the grid is usually referred to as a $\boldsymbol{K}$–orthogonal grid. Since

$$\boldsymbol{D} = \begin{bmatrix} x_{\hat{x}} & x_{\hat{y}} \\ y_{\hat{x}} & x_{\hat{y}} \end{bmatrix} = [\boldsymbol{x}_{21} + \boldsymbol{\omega}\hat{y}, \boldsymbol{x}_{41} + \boldsymbol{\omega}\hat{x}] \stackrel{\text{def}}{=} [\boldsymbol{\xi}_1(\hat{y}), \boldsymbol{\xi}_2(\hat{x})], \tag{2.3}$$

with $\boldsymbol{\omega} = (\boldsymbol{x}_{32} - \boldsymbol{x}_{41})$, we have

$$\hat{\boldsymbol{K}}^{-1} = \frac{1}{J}\begin{bmatrix} \boldsymbol{\xi}_1^T(\hat{y})\boldsymbol{K}^{-1}\boldsymbol{\xi}_1(\hat{y}) & \boldsymbol{\xi}_1^T(\hat{y})\boldsymbol{K}^{-1}\boldsymbol{\xi}_2(\hat{x}) \\ \boldsymbol{\xi}_2^T(\hat{x})\boldsymbol{K}^{-1}\boldsymbol{\xi}_1(\hat{y}) & \boldsymbol{\xi}_2^T(\hat{x})\boldsymbol{K}^{-1}\boldsymbol{\xi}_2(\hat{x}) \end{bmatrix}, \tag{2.4}$$

where the Jacobian is given by

$$\begin{aligned} J =& (x_{21}y_{41} - x_{41}y_{21}) + (x_{21}(y_{32} - y_{41}) - (x_{32} - x_{41})y_{21})\hat{x} \\ &+ ((x_{32} - x_{41})y_{41} - x_{41}(y_{32} - y_{41}))\hat{y}. \end{aligned} \tag{2.5}$$

Unless the grid consists of parallelogram cells, J and $\boldsymbol{D}$ will not be constant.

The grids is said to be h^2–*uniform* or asymptotic parallelogram grids, if there exits a constant c, independent of h, such that

$$|F_{\hat{x}\hat{y}}| = |\boldsymbol{\omega}| \leq ch^2.$$

This assumption is essential for the previous analysis given in [17], but will not be assumed here. Instead we need a less restrictive condition on the skewness of the cells uniformly on $\mathcal{T}_h$. This condition is defined below in Section 3.3. General quadrilateral grids without any asymptotic refinement condition on $\mathcal{T}_h$ is referred to as *rough grids*.

3. The Mixed Formulation of MPFA. Introduce the unknown velocity $\boldsymbol{u} = -\boldsymbol{K}\,\mathrm{grad}\,p$ which leads to a mixed formulation of equation (1.1). A weak formulation of (1.1) can then be the problem of finding $(\boldsymbol{u}, p) \in H(\mathrm{div}) \times \mathcal{L}_2$ such that

$$\begin{aligned} (\boldsymbol{K}^{-1}\boldsymbol{u}, \boldsymbol{v}) - (p, \mathrm{div}\,\boldsymbol{v}) &= 0, \qquad && \text{for all } \boldsymbol{v} \in H(\mathrm{div}), \\ (\mathrm{div}\,\boldsymbol{u}, q) &= (g, q), && \text{for all } q \in \mathcal{L}_2, \end{aligned} \tag{3.1}$$

where g is assumed to be an $\mathcal{L}_2$-function. With suitable discrete subspaces of $H(\mathrm{div})$ and $\mathcal{L}_2$, as well as a quadrature rule for $(\boldsymbol{K}^{-1}\boldsymbol{u}, \boldsymbol{v})$, the discrete version of (3.1) gives the physical space derived MPFA method of [2]. A direct derivation of MPFA and the equivalence to the discrete version of (3.1) is given in the Appendix.

3.1. The Broken Raviart-Thomas Element. We will create finite elements built on the broken Raviart-Thomas elements introduced and analyzed in [16, 17]. Let a, b, c, and d be piecewise constant on $(0,1)$, with discontinuity at the midpoint. On the reference square $\hat{E}$ the velocity space $\mathcal{RT}^{1/2} = \mathcal{RT}^{1/2}(\hat{E})$ on quadrilaterals is defined as the eight–dimensional space given as all vector fields of the form

$$\begin{bmatrix} a(\hat{y}) + b(\hat{y})\hat{x} \\ c(\hat{x}) + d(\hat{x})\hat{y} \end{bmatrix}.$$

Recall that the corresponding Raviart-Thomas space, $\mathcal{RT}$, is of the same form, but with, a, b, c, and d taken as constants, so $\mathcal{RT} \subset \mathcal{RT}^{1/2}$. The corresponding finite element space, $\mathcal{RT}_h^{1/2} \subset H(\mathrm{div})$, is now defined by

$$\mathcal{RT}_h^{1/2} := \{\boldsymbol{v} \in H(\mathrm{div}) : \ \boldsymbol{v}|_E \in \mathcal{P}_E(\mathcal{RT}^{1/2}), \quad \forall E \in \mathcal{T}_h\}.$$

Hence, the canonical degrees of freedom for the space $\mathcal{RT}_h^{1/2}$ are $\boldsymbol{v}\cdot\boldsymbol{n}$ of each half edge in $\mathcal{E}_h^{1/2}$. The classical $\mathcal{RT}_h$-elements, are defined similarly without any discontinuity. The pressure will be approximated by piecewise constants on

$$Q_h := \{q \in \mathcal{L}_2 : \ q|_E \in P_0(E), \quad \forall E \in \mathcal{T}_h\}.$$

On the reference element we define $\hat{\Pi} : (H^1(\hat{E}))^2 \to \mathcal{RT}$ as the standard interpolation operators onto the four dimensional Raviart–Thomas space, cf. [10],

$$\int_{\hat{e}} (\hat{\boldsymbol{u}} - \hat{\Pi}\hat{\boldsymbol{u}}) \cdot \hat{\boldsymbol{n}}\, d\hat{s} = 0, \text{ for all edges } \hat{e} \in \mathcal{E}(\hat{E}),$$

where $\mathcal{E}(\hat{E})$ represent the four edges of $\hat{E}$. The operator $\Pi_h : (H^1)^2 \to \mathcal{RT}_h \subset \mathcal{RT}_h^{1/2}$ is then simply given by

$$\Pi_h \boldsymbol{v}|_E = \mathcal{P}_E \hat{\Pi} \mathcal{P}_E^{-1} \boldsymbol{v}.$$

It is straightforward to check, using the identity (2.2), that the operator Π_h satisfies the identity

$$(\mathrm{div}(\Pi_h \boldsymbol{v} - \boldsymbol{v}), q) = 0, \qquad \text{for all } \boldsymbol{v} \in H(\mathrm{div}),\ q \in Q_h. \tag{3.2}$$

Note that the operator Π_h is well–defined on $\mathcal{RT}_h^{1/2}$ as well. By equivalence of norms we have

$$\|\Pi_h \boldsymbol{v}\| \le c\|\boldsymbol{v}\|, \quad \text{for all } \boldsymbol{v} \in \mathcal{RT}_h^{1/2}, \tag{3.3}$$

where the constant c is independent of h.

We also need the projection R_h defined on each cell E, as $R_h|_E = \mathcal{P}_E \hat{R}_E \mathcal{P}_E^{-1}$, for all $\boldsymbol{v} \in (H^1)^2$ such that

$$\hat{R}_E \hat{\boldsymbol{v}} = \hat{\Pi}\hat{\boldsymbol{v}} + \frac{\mathrm{div}\,\hat{\Pi}\hat{\boldsymbol{v}}}{2J_c} \begin{bmatrix} (J_2 - J_1)\hat{x}(\hat{x} - 1) \\ (J_4 - J_1)\hat{y}(\hat{y} - 1) \end{bmatrix} \tag{3.4}$$

where $J_i = J(\hat{\boldsymbol{x}}_i)$, $i = 1, 2, 3, 4$ is the Jacobian evaluated in the reference cell vertex, and $J_c = J(1/2, 1/2)$ the Jacobian evaluated in the reference cell center. Note that $J_c = \sum J_i/4$. With this notation equation (2.5) can be written

$$J = J_1 + (J_2 - J_1)\hat{x} + (J_4 - J_1)\hat{y}. \tag{3.5}$$

On each cell E, from relation (2.2) and (3.5)

$$\begin{aligned}\operatorname{div}(R_h\boldsymbol{v})J &= \operatorname{div}(\hat{R}_E\hat{\boldsymbol{v}}) \\ &= \operatorname{div}(\hat{\Pi}\hat{\boldsymbol{v}}) + \frac{\operatorname{div}(\hat{\Pi}\hat{\boldsymbol{v}})}{2J_c}((J_2-J_1)(2\hat{x}-1)+(J_4-J_1)(2\hat{y}-1)) \\ &= \frac{\operatorname{div}(\hat{\Pi}\hat{\boldsymbol{v}})}{J_c}(J_1+(J_2-J_1)\hat{x}+(J_4-J_1)\hat{y}) \\ &= \frac{\operatorname{div}(\hat{\Pi}\hat{\boldsymbol{v}})}{J_c}J.\end{aligned}$$

The construction in (3.4) therefore ensures $\operatorname{div} R_h\boldsymbol{v} = \operatorname{div}(\hat{\Pi}\hat{\boldsymbol{v}})/J_c \in P_0(E), \forall E \in \mathcal{T}_h$. Note that $R_h\boldsymbol{v} \notin \mathcal{RT}_h$, but the second therm of (3.4) vanish on the cell boundary, such that it follows from (3.2) that also

$$(\operatorname{div}(R_h\boldsymbol{v}-\boldsymbol{v}),q) = 0, \qquad \text{for all } \boldsymbol{v} \in H(\operatorname{div}),\ q \in Q_h. \tag{3.6}$$

If $\mathcal{M}_h$ is the $\mathcal{L}_2$–projection onto Q_h, we now have $\operatorname{div} R_h = \mathcal{M}_h \operatorname{div}$. The projection R_h is motivated from the $\mathcal{ABF}_0$ elements introduced in [7], and allows us to find a convergence estimate of the divergence without assuming h^2-uniform grids.

The mixed finite element method derived from the pair $\mathcal{RT}_h^{1/2} \times Q_h$ is given by: Find $(\boldsymbol{u}_h, p_h) \in \mathcal{RT}_h^{1/2} \times Q_h \subset H(\operatorname{div}) \times \mathcal{L}_2$ such that

$$\begin{aligned}(\boldsymbol{K}^{-1}\boldsymbol{u}_h,\boldsymbol{v}) - (p_h, \operatorname{div}\boldsymbol{v}) &= 0, \qquad && \text{for all } \boldsymbol{v} \in \mathcal{RT}_h^{1/2}, \\ (\operatorname{div}\boldsymbol{u}_h, q) &= (g,q), && \text{for all } q \in Q_h.\end{aligned} \tag{3.7}$$

In order to obtain the MPFA method as a mixed finite element method we need to replace the term $(\boldsymbol{K}^{-1}\boldsymbol{u}_h,\boldsymbol{v})_E$ in (3.7) by a quadrature formula.

3.2. The Quadrature Rule. Let $\boldsymbol{K}_h^{-1}$ denote the $\mathcal{L}_2$-projection of the components of $\boldsymbol{K}^{-1}$ onto $P_0(E)$ for all $E \in \mathcal{T}_h$. Since the components of $\boldsymbol{K}^{-1}$ are C^1 there exists a constant c independent of h such that

$$|((\boldsymbol{K}_h^{-1}-\boldsymbol{K}^{-1})\boldsymbol{u},\boldsymbol{v})| \le ch\|\boldsymbol{u}\|\|\boldsymbol{v}\|, \tag{3.8}$$

for $\boldsymbol{u},\boldsymbol{v} \in (\mathcal{L}_2)^2$. For a general function $\phi(\hat{\boldsymbol{x}}) \in \mathcal{L}_2$ on a unit square $\hat{E}$, with vertices $\hat{\boldsymbol{x}}_i = (0,0)$, $(1,0)$, $(1,1)$ and $(0,1)$ for $i = 1,2,3,4$, let approximation of the integral of ϕ by the trapezoidal rule mean that

$$\int_{\hat{E}} \phi(\hat{\boldsymbol{x}})\, d\hat{\boldsymbol{x}} \approx T_{\hat{E}}(\phi) = \frac{1}{4}\sum_{i=1}^{4}\phi(\hat{\boldsymbol{x}}_i).$$

Let the subscript c denote evaluation in the reference cell center, $\hat{\boldsymbol{x}}_c$, so $\boldsymbol{D}_c = \boldsymbol{D}(\hat{\boldsymbol{x}}_c)$ for all cells. Now, define our numerical quadrature formula on each cell $E \in \mathcal{T}_h$ such that

$$a_E(\boldsymbol{u},\boldsymbol{v}) = T_{\hat{E}}(\frac{1}{J}\boldsymbol{D}_c^T\boldsymbol{K}_h^{-1}\boldsymbol{D}\,\hat{\boldsymbol{u}}\cdot\hat{\boldsymbol{v}}) \tag{3.9}$$

with

$$a_h(\boldsymbol{u},\boldsymbol{v}) = \sum_{\mathcal{T}_h} a_E(\boldsymbol{u},\boldsymbol{v}), \tag{3.10}$$

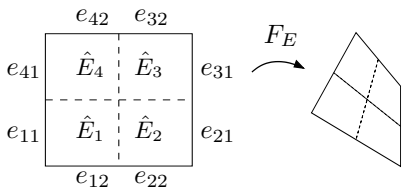

FIG. 3.1. *One cell, with four subcells, and the half cell edges* e_{ij}.

for piecewise smooth vector fields $\boldsymbol{u}$ and $\boldsymbol{v}$. Note that the bilinear form a_h is non symmetric due to the fact that one of the Jacobian matrices $\boldsymbol{D}$ appearing in (3.9) is evaluated at the reference cell center, $\hat{\boldsymbol{x}}_c$. The motivation for this construction is the need to fulfill the properties given in Lemma 3.1 below. These properties are expressed directly on the physical cell E, and thereby inherit the non symmetry from the non parallel edge vectors of E.

Divide each cell into four subcells E_i created by a line between the edge midpoints, cf Figure 3.1. The approximation of $\hat{\boldsymbol{K}}^{-1}$ on each subcell $\hat{E}_i$ can now be described by the non symmetric matrix

$$\Lambda_{E_i} = \frac{1}{J_i} \boldsymbol{D}_c^T \boldsymbol{K}_h^{-1} \boldsymbol{D}_i, \tag{3.11}$$

with $J_i = J(\hat{\boldsymbol{x}}_i)$ and $\boldsymbol{D}_i = \boldsymbol{D}(\hat{\boldsymbol{x}}_i)$. Let e_{ij} denote the outer half edge of subcell $\hat{E}_i$ with the jth unit vector as a normal, cf. Figure 3.1. Note that if $\hat{\boldsymbol{v}} = (\hat{v}_1, \hat{v}_2) \in \mathcal{RT}^{1/2}$ the exactness of the trapezoidal rule for scalar linear functions implies that

$$\sum_{i=1}^{4} \hat{v}_j|_{e_{ij}} = \int_{\hat{E}} \hat{v}_j d\hat{\boldsymbol{x}}, \qquad k = 1, 2,$$

or with $\boldsymbol{\phi} \in (P_0(\hat{E}))^2$

$$T_{\hat{E}}(\boldsymbol{\phi} \cdot \hat{\boldsymbol{v}}) = (\boldsymbol{\phi}, \hat{\boldsymbol{v}})_{\hat{E}}. \tag{3.12}$$

Since $\hat{\Pi}\hat{\boldsymbol{v}}$ on an edge is the average of the two $\hat{\boldsymbol{v}}$ values on each half edge, we also have

$$T_{\hat{E}}(\boldsymbol{\phi} \cdot (\hat{\boldsymbol{v}} - \hat{\Pi}\hat{\boldsymbol{v}})) = 0. \tag{3.13}$$

Let $\hat{v}_j|_{e_{ij}} = \hat{v}_{ij} = v_{ij}$, then for $\boldsymbol{v}, \boldsymbol{u} \in \mathcal{RT}_h^{1/2}$ (3.9) and (3.10) can be rewritten as

$$a_h(\boldsymbol{u}, \boldsymbol{v}) = \frac{1}{4} \sum_{i=1}^{4} \sum_{j,k=1}^{2} \kappa_{jk}^{E_i} u_{ij} v_{ik} \tag{3.14}$$

where $\kappa_{jk}^{E_i}$ are components of the non symmetric matrix Λ_{E_i}, cf. (3.11). Due to the linearity of $\boldsymbol{D}$ cf. (2.3), we also have for all $\boldsymbol{v} = (v_1(\hat{x}), v_2(\hat{y})) \in \mathcal{RT}_h$

$$\int_{\hat{E}} \boldsymbol{D}_c \hat{\boldsymbol{v}}\, d\hat{\boldsymbol{x}} = \int_{\hat{E}} \boldsymbol{\xi}_1(\hat{y}) v_1(\hat{x}) + \boldsymbol{\xi}_2(\hat{x}) v_2(\hat{y}) d\hat{\boldsymbol{x}} = \int_{\hat{E}} \boldsymbol{D}\hat{\boldsymbol{v}}\, d\hat{\boldsymbol{x}}. \tag{3.15}$$

The following Lemma is a key result for the bilinear form a_h. In [17] analogous results are stated on the reference space.

LEMMA 3.1. *If* $\boldsymbol{u} \in (P_0(E))^2$, *the quadrature rule defined by* (3.14) *satisfies*

$$a_E(\boldsymbol{u}, \boldsymbol{v} - \Pi_h \boldsymbol{v}) = 0 \qquad \textit{for all } \boldsymbol{v} \in \mathcal{RT}_h^{1/2}, \tag{3.16}$$

and

$$a_E(\boldsymbol{u},\boldsymbol{v}) = (\boldsymbol{K}_h^{-1}\boldsymbol{u},\boldsymbol{v})_E \qquad \textit{for all } \boldsymbol{v}\in\mathcal{RT}_h. \tag{3.17}$$

Proof. To prove (3.16), note that for $\boldsymbol{u}\in(P_0(E))^2$, $\hat{\boldsymbol{u}} = J\boldsymbol{D}^{-1}\boldsymbol{u}\in\mathcal{RT}(\hat{E})$, and for $\boldsymbol{v}\in\mathcal{RT}_h^{1/2}$ it follows from (3.9) and (3.13) that

$$\begin{aligned} a_E(\boldsymbol{u},\boldsymbol{v}-\Pi_h\boldsymbol{v}) &= T_{\hat{E}}(\frac{1}{J}\boldsymbol{D}_c^T\boldsymbol{K}_h^{-1}\boldsymbol{D}\,J\boldsymbol{D}^{-1}\boldsymbol{u}\cdot(\hat{\boldsymbol{v}}-\hat{\Pi}\hat{\boldsymbol{v}}))\\ &= T_{\hat{E}}(\boldsymbol{D}_c^T\boldsymbol{K}_h^{-1}\boldsymbol{u}\cdot(\hat{\boldsymbol{v}}-\hat{\Pi}\hat{\boldsymbol{v}}))\\ &= 0, \end{aligned}$$

since $\boldsymbol{D}_c^T\boldsymbol{K}_h^{-1}\boldsymbol{u}\in(P_0(\hat{E}))^2$. Similarly, for all $\boldsymbol{v}\in\mathcal{RT}_h^{1/2}$ we obtain from (3.12) that

$$\begin{aligned} a_E(\boldsymbol{u},\boldsymbol{v}) &= T_{\hat{E}}(\boldsymbol{D}_c^T\boldsymbol{K}_h^{-1}\boldsymbol{u}\cdot\hat{\boldsymbol{v}})\\ &= (\boldsymbol{D}_c^T\boldsymbol{K}_h^{-1}\boldsymbol{u},\hat{\boldsymbol{v}})_{\hat{E}}. \end{aligned}$$

Further, since $\boldsymbol{K}_h^{-1}\boldsymbol{u}\in(P_0(\hat{E}))^2$, it follows from (3.15) that

$$\begin{aligned} (\boldsymbol{K}_h^{-1}\boldsymbol{u},\boldsymbol{D}_c\hat{\boldsymbol{v}})_{\hat{E}} &= (\boldsymbol{K}_h^{-1}\boldsymbol{u},\boldsymbol{D}\hat{\boldsymbol{v}})_{\hat{E}}\\ &= (\boldsymbol{K}_h^{-1}\boldsymbol{u},\boldsymbol{v})_E \end{aligned}$$

for all $\boldsymbol{v}\in\mathcal{RT}_h$. This shows the exactness of equation (3.17). □

The method of our interest, is the solution $(\boldsymbol{u}_h,p_h)\in\mathcal{RT}_h^{1/2}\times Q_h$ such that

$$\begin{aligned} a_h(\boldsymbol{u}_h,\boldsymbol{v}) - (p_h,\operatorname{div}\boldsymbol{v}) &= 0, \qquad && \text{for all } \boldsymbol{v}\in\mathcal{RT}_h^{1/2},\\ (\operatorname{div}\boldsymbol{u}_h,q) &= (g,q), && \text{for all } q\in Q_h. \end{aligned} \tag{3.18}$$

To ensure uniqueness of this system we require the symmetric part of a_h to be coercive. This follows if the symmetric part of Λ, (3.11), is uniformly positive definite, see the discussion in Section 3.3 below.

The effect of the broken Raviart-Thomas elements and the quadrature rule is a block diagonal mass matrix. The block structure corresponds to dual cells, consisting of subcells with a common vertex. Inverting the local blocks enables us to find a discrete explicit flux for each half edge, which can be used in a control volume formulation. In the Appendix, Theorem A.2, the exact correspondence between the expression (3.18), and the classical MPFA derived in the physical space as found in for instance [2] is shown.

3.3. Handling the Non Symmetry. In order to analyze the mixed method (3.18) we also need some properties of the bilinear form a_h defined on the space $\mathcal{RT}_h^{1/2}$. Recall the definition of the matrix Λ from (3.11), which is coefficients of a_h, cf. (3.14). The matrix Λ is bounded uniformly in h. To ensure coercivity of a_h, we assume $\Lambda+\Lambda^T$ to be uniformly positive definite on $\mathcal{T}_h$. Throughout the rest of this paper we assume

$$\det(\Lambda+\Lambda^T)\geq\gamma_0, \tag{3.19}$$

to hold on all subcells with a constant $\gamma_0>0$ independent of h.

This condition measure the skewness of the cell wighted by $\boldsymbol{K}$. To illustrate the condition, we assume $\boldsymbol{K}$ to be the identity I. Then (3.19) demands the inner-product of the logically horizontal and vertically edge vector to dominate the cross inner-product of these vectors, cf. (2.4), (3.11) and Figure 3.2-(i), such that

$$(\boldsymbol{\xi}_{1,i}\cdot\boldsymbol{\xi}_{1,c})(\boldsymbol{\xi}_{2,i}\cdot\boldsymbol{\xi}_{2,c}) - ((\boldsymbol{\xi}_{1,i}\cdot\boldsymbol{\xi}_{2,c}+\boldsymbol{\xi}_{1,c}\cdot\boldsymbol{\xi}_{2,i})/2)^2 \geq J_i\gamma_0.$$

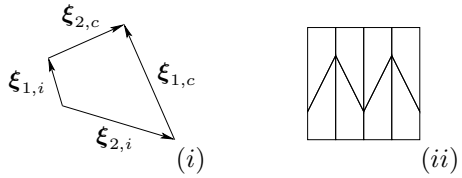

FIG. 3.2. (i) *A subcell, and it's edge vectors.* (ii) *Zigzag grid, with 1:3 cell edge length.*

Note that the first term here always is positive, since the angle between the opposite subcell edges is bounded by $\pi/2$, from the subcell construction and regularity of $\mathcal{T}_h$. The condition (3.19) will for example hold on the trapezoidal or zigzag grids of [7] with $\boldsymbol{K} = I$. Even rougher cells with $\boldsymbol{x}_{21} = (h, 0)$, $\boldsymbol{x}_{41} = (0, h)$ and $\boldsymbol{x}_{32} = (0, 3h)$, cf. Figure 3.2-$(ii)$, satisfies (3.19), if $\boldsymbol{K} = I$. Note that this condition is independent of h, and holds on rough quadrilateral grids without any asymptotic refinement condition on $\mathcal{T}_h$.

Using the regularity of the mesh, the assumption (3.19), and the equivalence of norms on the reference element $\hat{E}$ it is straightforward to show that $a_h(\boldsymbol{v}, \boldsymbol{v})^{1/2}$ is equivalent to the $\mathcal{L}_2$ norm on $\mathcal{RT}_h^{1/2}$, i.e. there are constants $\alpha_0, \alpha_1 > 0$, independent of h, such that

$$\alpha_0 \|\boldsymbol{v}\|^2 \leq a_h(\boldsymbol{v}, \boldsymbol{v}) \leq \alpha_1 \|\boldsymbol{v}\| \|\boldsymbol{u}\|. \tag{3.20}$$

The upper bound holds since $\boldsymbol{D}_c \boldsymbol{D}^{-1}$ is uniformly bounded. From the lower bound, the uniqueness of (3.18) now follows.

4. Convergence of the MPFA. In this final section of the paper we show the convergence of the MPFA system (3.18).

LEMMA 4.1. *Let* $\boldsymbol{v} \in (H^1)^2$, *with* $\operatorname{div} \boldsymbol{v} \in H^1$ *and* $p \in H^1$. *Further let* $\mathcal{M}_h$ *be the* $\mathcal{L}_2$*–projection onto* Q_h, *and* $\Pi_{0,h}$ *the* $\mathcal{L}_2$*–projection onto* $(P_0(E))^2$ *for all* $E \in \mathcal{T}_h$. *Then there is a constant* c, *independent of* h, *such that*

$$\|\mathcal{M}_h p - p\| \leq ch\|p\|_1, \tag{4.1}$$
$$\|\Pi_{0,h} \boldsymbol{v} - \boldsymbol{v}\| \leq ch\|\boldsymbol{v}\|_1, \tag{4.2}$$
$$\|\Pi_h \boldsymbol{v} - \boldsymbol{v}\| \leq ch\|\boldsymbol{v}\|_1, \tag{4.3}$$
$$\|\operatorname{div}(R_h \boldsymbol{v} - \boldsymbol{v})\| \leq ch\|\operatorname{div} \boldsymbol{v}\|_1, \tag{4.4}$$

Proof. Inequalities (4.1) and (4.2) follows by ordinary interpolation estimates. Inequality (4.3) can be found in [7]. Since $\operatorname{div} R_h \boldsymbol{v} = \mathcal{M}_h \operatorname{div} \boldsymbol{v}$, cf. (3.6), (4.4) follows from (4.1). □

LEMMA 4.2. *Let* $\boldsymbol{u} \in (H^1)^2$ *and* $\boldsymbol{v} \in \mathcal{RT}_h^{1/2}$. *Then there is a constant* c, *independent of* h, *such that*

$$|a_h(\Pi_h \boldsymbol{u}, (I - \Pi_h)\boldsymbol{v})| \leq ch\|\boldsymbol{u}\|_1 \|(I - \Pi_h)\boldsymbol{v}\|.$$

Proof. From Lemma 3.1, we have

$$a_E(\Pi_{0,h} \boldsymbol{u}, (\boldsymbol{v} - \Pi_h \boldsymbol{v})) = 0.$$

From Lemma 4.1, (4.2) and (3.20) we obtain

$$\begin{aligned} a_E(\Pi_h \boldsymbol{u}, (I-\Pi_h)\boldsymbol{v}) &= |a_E((\Pi_h - \Pi_{0,h})\boldsymbol{u}, (I-\Pi_h)\boldsymbol{v})| \\ &\le \alpha_1 \|(\Pi_h - \Pi_{0,h})\boldsymbol{u}\|_E \|(I-\Pi_h)\boldsymbol{v}\|_E \\ &\le ch\|\boldsymbol{u}\|_{1,E}\|(I-\Pi_h)\boldsymbol{v}\|_E. \end{aligned}$$

Summing over $\mathcal{T}_h$, the desired result follows. □

Let $a(\boldsymbol{u},\boldsymbol{v})$ be the continuous bilinear form $(\boldsymbol{K}^{-1}\boldsymbol{u},\boldsymbol{v})$. The next result is a consistency result for the bilinear form a_h.

LEMMA 4.3. *Let $\boldsymbol{u} \in (H^1)^2$ and $\boldsymbol{v} \in \mathcal{RT}_h$. Then there is a constant c, independent of h, such that*

$$|a_h(\Pi_h \boldsymbol{u}, \boldsymbol{v}) - a(\boldsymbol{u},\boldsymbol{v})| \le ch\|\boldsymbol{u}\|_1 \|\boldsymbol{v}\|.$$

Proof. From Lemmas 3.1 and 4.1, the boundedness of a and (3.8) we derive

$$\begin{aligned} &|a_h(\Pi_h \boldsymbol{u}, \boldsymbol{v}) - a(\boldsymbol{u},\boldsymbol{v})| \\ &\quad = |\, a_h((\Pi_h - \Pi_{0,h})\boldsymbol{u}, \boldsymbol{v}) + ((\boldsymbol{K}_h^{-1} - \boldsymbol{K}^{-1})\Pi_{0,h}\boldsymbol{u}, \boldsymbol{v}) + a((\Pi_{0,h} - I)\boldsymbol{u}, \boldsymbol{v})| \\ &\quad \le c\left(\|\Pi_h \boldsymbol{u} - \boldsymbol{u}\| + \|\Pi_{0,h}\boldsymbol{u} - \boldsymbol{u}\| + h\|\Pi_{0,h}\boldsymbol{u}\|\right)\|\boldsymbol{v}\| \\ &\quad \le ch\|\boldsymbol{u}\|_1\|\boldsymbol{v}\|. \end{aligned}$$

□

Remark. Lemma 4.2 and 4.3 are stated in the physical space. To achieve this statements in the physical space we essentially used that one of the Jacobian matrix was evaluated in the cell center, cf. (3.9) and Lemma 3.1, which again caused the non symmetry of the method. □

It is well known that, in addition to the boundedness of the bilinear forms, two corresponding Brezzi conditions have to be satisfied in order to ensure stability of a mixed finite element method of the form (3.18), cf. [10]. For the continuous mixed formulation (3.1) the proper function space for the formulation is $H(\mathrm{div}) \times \mathcal{L}_2$. Hence, in the present setting the first Brezzi condition requires that

$$\sup_{\boldsymbol{v} \in \mathcal{RT}_h^{1/2}} \frac{(q, \mathrm{div}\, \boldsymbol{v})}{\|\boldsymbol{v}\|_{\mathrm{div}}} \ge \beta_1 \|q\| \qquad \text{for all } q \in Q_h, \tag{4.5}$$

where $\beta_1 > 0$ is independent of h. Since $\mathcal{RT}_h^{1/2} \supset \mathcal{RT}_h$, and the corresponding condition is well known to hold for the pair $\mathcal{RT}_h \times Q_h$, cf. [10, 18], we conclude that (4.5) is fulfilled.

The second stability condition is related to the weakly divergence free vector fields in $\mathcal{RT}_h^{1/2}$. Let Z_h denote the set of weakly divergence free vector fields, i.e.

$$Z_h = \{\boldsymbol{v} \in \mathcal{RT}_h^{1/2} : (\mathrm{div}\, \boldsymbol{v}, q) = 0, \quad \forall q \in Q_h\}.$$

The standard formulation of the second stability condition states that

$$\|\boldsymbol{v}\|_{\mathrm{div}} \le \beta_2 \|\boldsymbol{v}\| \qquad \text{for all } \boldsymbol{v} \in Z_h,$$

where β_2 is independent of h. This condition does not hold in the present case since the elements of Z_h are not divergence free. However, if $\boldsymbol{v} \in Z_h \cap \mathcal{RT}_h$ then $\mathrm{div}\, v = 0$.

This is seen by a transformation back to the reference space. Hence, for any $\boldsymbol{v} \in Z_h$ we must have that $\operatorname{div} \hat{\Pi}\hat{\boldsymbol{v}} = 0$ and it follows that $\operatorname{div} R_E \boldsymbol{v} = 0$. Therefore, the weaker condition

$$\|\boldsymbol{v}\| + \|\operatorname{div} R_h \boldsymbol{v}\| \leq \beta_2 \|\boldsymbol{v}\| \qquad \text{for all } \boldsymbol{v} \in Z_h,$$

holds with constant $\beta_2 = 1$. This slight lack of stability for the mixed method (3.18) will have consequences for the error estimates we shall obtain. Instead of estimates in the norm of $H(\operatorname{div}) \times \mathcal{L}_2$ we will instead obtain estimates in a weaker norm.

Let $(\boldsymbol{u}, p) \in H(\operatorname{div}) \times \mathcal{L}_2$ be the solution of the continuous problem (3.1) and $(\boldsymbol{u}_h, p_h) \in \mathcal{RT}_h^{1/2} \times Q_h$ the corresponding solution of (3.18). We assume that $\boldsymbol{u}$, $\operatorname{div} \boldsymbol{u}$, and p are all H^1 functions. Note that it follows from (3.2) that $\Pi_h(\boldsymbol{u} - \boldsymbol{u}_h) \in Z_h \cap \mathcal{RT}_h$ and therefore $\operatorname{div} \Pi_h(\boldsymbol{u} - \boldsymbol{u}_h) = 0$ and also $\operatorname{div} R_h(\boldsymbol{u} - \boldsymbol{u}_h) = 0$. We can therefore conclude from (4.4), that

$$\|\operatorname{div}(\boldsymbol{u} - R_h \boldsymbol{u}_h)\| = \|\operatorname{div}(\boldsymbol{u} - R_h \boldsymbol{u})\| \leq ch \|\operatorname{div} \boldsymbol{u}\|_1. \tag{4.6}$$

The $\mathcal{L}_2$ norm of $\boldsymbol{u} - \boldsymbol{u}_h$ is estimated next.

LEMMA 4.4. *There is a constant c, independent of h, such that*

$$\|\boldsymbol{u} - \boldsymbol{u}_h\| \leq ch \|\boldsymbol{u}\|_1.$$

Proof. Due to the interpolation result (4.3) it is enough to show that

$$\|\Pi_h \boldsymbol{u} - \boldsymbol{u}_h\| \leq ch \|\boldsymbol{u}\|_1. \tag{4.7}$$

Furthermore, by (3.20) it is sufficient to estimate $a_h(\Pi_h \boldsymbol{u} - \boldsymbol{u}_h, \Pi_h \boldsymbol{u} - \boldsymbol{u}_h)^{1/2}$.

In order to do this we start by observing that since $\Pi_h(\boldsymbol{u} - \boldsymbol{u}_h)$ is divergence free it follows from the definition of $\boldsymbol{u}_h$ and (3.2) that

$$a_h(\boldsymbol{u}_h, \Pi_h \boldsymbol{u} - \boldsymbol{u}_h) = (p_h, \operatorname{div}(\Pi_h \boldsymbol{u} - \boldsymbol{u}_h)) = (p_h, \operatorname{div} \Pi_h(\boldsymbol{u} - \boldsymbol{u}_h)) = 0.$$

Hence,

$$\begin{aligned} a_h(\Pi_h \boldsymbol{u} - \boldsymbol{u}_h, \Pi_h \boldsymbol{u} - \boldsymbol{u}_h) &= a_h(\Pi_h \boldsymbol{u}, \Pi_h \boldsymbol{u} - \boldsymbol{u}_h) \\ &= a_h(\Pi_h \boldsymbol{u}, \Pi_h(\boldsymbol{u} - \boldsymbol{u}_h)) - a_h(\Pi_h \boldsymbol{u}, (I - \Pi_h)\boldsymbol{u}_h). \end{aligned}$$

Since

$$a(\boldsymbol{u}, \Pi_h(\boldsymbol{u} - \boldsymbol{u}_h)) = (p, \operatorname{div}(\Pi_h(\boldsymbol{u} - \boldsymbol{u}_h))) = 0,$$

we obtained the identity

$$a_h(\Pi_h \boldsymbol{u} - \boldsymbol{u}_h, \Pi_h \boldsymbol{u} - \boldsymbol{u}_h) = [a_h(\Pi_h \boldsymbol{u}, \Pi_h(\boldsymbol{u} - \boldsymbol{u}_h)) - a(\boldsymbol{u}, \Pi_h(\boldsymbol{u} - \boldsymbol{u}_h))] - a_h(\Pi_h \boldsymbol{u}, (I - \Pi_h)\boldsymbol{u}_h).$$

From the estimates of the Lemmas 4.2 and 4.3 we derive

$$\begin{aligned} a_h(\Pi_h \boldsymbol{u} - \boldsymbol{u}_h, \Pi_h \boldsymbol{u} - \boldsymbol{u}_h) &\leq ch \|\boldsymbol{u}\|_1 (\|\Pi_h(\boldsymbol{u} - \boldsymbol{u}_h)\| + \|(I - \Pi_h)\boldsymbol{u}_h\|) \\ &\leq ch \|\boldsymbol{u}\|_1 \|\Pi_h \boldsymbol{u} - \boldsymbol{u}_h\|, \end{aligned}$$

where the final inequality follows from (3.3). By (3.20) this implies (4.7). ∎

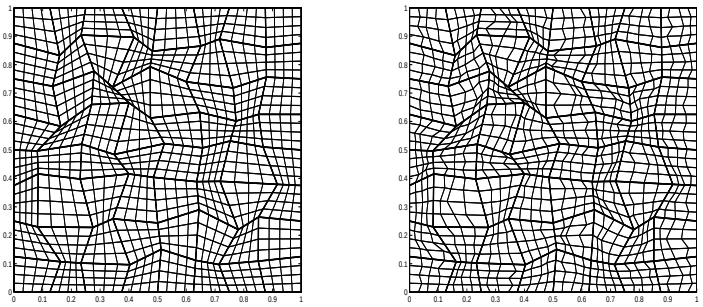

FIG. 5.1. *To the left an initial randomly generated grid, refined under the h^2-uniform condition. To the right the refinement is continued to be randomly generated.*

For the final estimate on $\|p - p_h\|$ it is, by (4.1), enough to bound $\|\mathcal{M}_h p - p_h\|$. The inf–sup condition on $\mathcal{RT}_h \times Q_h$ gives

$$\begin{aligned}
\|\mathcal{M}_h p - p_h\| \leq & c \sup_{\boldsymbol{v} \in \mathcal{RT}_h} \frac{(\mathcal{M}_h p - p_h, \operatorname{div} \boldsymbol{v})}{\|\boldsymbol{v}\|_{\operatorname{div}}} \\
\leq & c \left\{ \|\mathcal{M}_h p - p\| + \sup_{\boldsymbol{v} \in \mathcal{RT}_h} \frac{(p - p_h, \operatorname{div} \boldsymbol{v})}{\|\boldsymbol{v}\|_{\operatorname{div}}} \right\} \\
\leq & c \left\{ \|\mathcal{M}_h p - p\| + \sup_{\boldsymbol{v} \in \mathcal{RT}_h} \frac{|a(\boldsymbol{u}, \boldsymbol{v}) - a_h(\Pi_h \boldsymbol{u}, \boldsymbol{v})| + a_h(\Pi_h \boldsymbol{u} - \boldsymbol{u}_h, \boldsymbol{v})}{\|\boldsymbol{v}\|_{\operatorname{div}}} \right\} \\
\leq & ch \left(\|p\|_1 + \|\boldsymbol{u}\|_1 \right)
\end{aligned}$$

where we have used (4.1), (4.7) and Lemma 4.3.

Together with (4.6) and Lemma 4.4 this implies the following set of error estimates for the MPFA method.

THEOREM 4.5. *Let $(\boldsymbol{u}, p)$ be the exact solution of (3.1) and $(\boldsymbol{u}_h, p_h) \subset \mathcal{RT}_h^{1/2} \times Q_h$ the solution of (3.18). If* (3.19) *hold on rough grids, there is a constant c, independent of h, but depending on $\|\boldsymbol{u}\|_1$, $\|\operatorname{div} \boldsymbol{u}\|_1$ and $\|p\|_1$, such that*

$$\|\boldsymbol{u}_h - \boldsymbol{u}\| + \|\operatorname{div}(R_h \boldsymbol{u}_h - \boldsymbol{u})\| + \|p_h - p\| \leq ch.$$

Remark. Recall that $\operatorname{div} \circ R_h$ maps $(H^1)^2$ into the piecewise constant space Q_h, and satisfies the commuting diagram property (3.6) i.e. $\operatorname{div} \circ R_h = \mathcal{M}_h \circ \operatorname{div}$. This ensures the convergence of the discrete divergence, cf. (4.4). The convergence results from Theorem 4.5, also apply to the classical Raviart-Thomas solution, cf. (3.7) with $(\boldsymbol{u}_h, p_h)$ and $(\boldsymbol{v}, q) \in \mathcal{RT}_h \times Q_h$. Therefore this gives convergence of the classical Raviart-Thomas method without performing the $\mathcal{ABF}_0$–modification of the finite element space. □

5. Numerical Experiments. Extensive numerical testing has been performed on the convergence of the physical space derived MPFA discretization, cf. [3, 4, 14]. The following example illustrates the good convergence qualities on rough grids for the physical space based MPFA compared to the reference space based version.

Let the eigenvalues for K be 10 and 1, such that the first eigenvector is tilted $\pi/6$

$$K = \begin{bmatrix} 7.7500 & 3.8971 \\ 3.8971 & 3.2500 \end{bmatrix}.$$

$1/h$	$\|p_h - p(\boldsymbol{x}_c)\|$	Rate	$\|\boldsymbol{u} - \Pi_h \boldsymbol{u}_h\|_h$	Rate	$\|\boldsymbol{u} - \boldsymbol{u}_h\|_h$	Rate
8	1.0757e-01	-	1.8941e+00	-	1.1895e+01	-
16	2.3886e-02	2.1711	5.6159e-01	1.7539	5.7213e+00	1.0560
32	5.6811e-03	2.0719	1.5173e-01	1.8880	2.8030e+00	1.0294
64	1.3895e-03	2.0316	3.9690e-02	1.9346	1.3864e+00	1.0157
128	3.4374e-04	2.0151	1.0227e-02	1.9563	6.8930e-01	1.0081

TABLE 5.1
h^2–uniform grids, physical space derived MPFA.

$1/h$	$\|p_h - p(\boldsymbol{x}_c)\|$	Rate	$\|\boldsymbol{u} - \Pi_h \boldsymbol{u}_h\|_h$	Rate	$\|\boldsymbol{u} - \boldsymbol{u}_h\|_h$	Rate
8	1.5182e-01	-	5.7974e+00	-	1.2972e+01	-
16	4.2602e-02	1.8334	1.9082e+00	1.6032	6.1824e+00	1.0692
32	1.0946e-02	1.9605	5.8892e-01	1.6960	3.0649e+00	1.0123
64	2.7444e-03	1.9958	1.6940e-01	1.7976	1.5288e+00	1.0034
128	6.8334e-04	2.0058	4.7211e-02	1.8433	7.6369e-01	1.0013

TABLE 5.2
h^2–uniform grids, reference space derived MPFA.

The boundary condition is then chosen to corresponds to

$$p(x, y) = \cos(2\pi x)\cos(2\pi y),$$

while

$$\boldsymbol{u} = -\boldsymbol{K}\,\mathrm{grad}\, p.$$

The velocity is measured in a discrete norm

$$\|\boldsymbol{u} - \boldsymbol{u}_h\|_h^2 = \sum_{j \in \mathcal{E}_h^{1/2}} (\boldsymbol{u}(\boldsymbol{x}_j) \cdot \boldsymbol{n}_j - u_j)^2 w_j,$$

where $w_j = (|E_{j+}| \bigcap |E_{j-}|)/8$ is the area associated with half edge j from the two adjacent cells E_{j+} and E_{j-}, and $\boldsymbol{x}_j$ is the midpoint of edge j. The convergence is checked for both the physical and reference space derived methods. For the reference space based method we evaluate $\hat{\boldsymbol{K}}$ in the cell centers. Other evaluation points, like the cell vertices, are also tested with similar results. We consider two grids shown in Figure 5.1. To the left an initial randomly generated grid is refined under the h^2-uniform condition, while to the right we have a rough grid, where the refinement is continued to be randomly generated. Both the physical and reference space derived methods converge on the h^2-uniform grids, cf. Table 5.1 and 5.2. The convergence rate for the pressure is for both cases $\mathcal{O}(h^2)$, while for the discrete velocities it is $\mathcal{O}(h)$. For the average of the half edge flux on each edge, $\Pi_h \boldsymbol{u}_h$, a superconvergence effect occurs and we get $\mathcal{O}(h^2)$ convergence. On the rough grids the reference space based method diverge, cf. Table 5.3. This is in agreement with the analysis in [17], where the h^2-uniform grid condition shows up. The robustness of the physical space derived method on these grids is shown, cf. Table 5.4. The grid condition (3.19) is violated for around 0.2% of the cells. The numerical experiments show close to $\mathcal{O}(h^2)$ convergence for the pressure, while we do not get any superconvergence effect for the velocity. Both $\boldsymbol{u}_h$ and $\Pi \boldsymbol{u}_h$ are of $\mathcal{O}(h)$.

$1/h$	$\|p_h - p(\boldsymbol{x}_c)\|$	Rate	$\|\boldsymbol{u} - \Pi_h \boldsymbol{u}_h\|_h$	Rate	$\|\boldsymbol{u} - \boldsymbol{u}_h\|_h$	Rate
8	1.5182e-01	-	5.7974e+00	-	1.2972e+01	-
16	4.7111e-02	1.6883	2.3935e+00	1.2763	6.3577e+00	1.0289
32	1.6289e-02	1.5322	1.6261e+00	0.5577	3.4695e+00	0.8738
64	8.5296e-03	0.9334	1.5232e+00	0.0944	2.2687e+00	0.6128
128	6.2829e-03	0.4411	1.5934e+00	-0.0651	1.9526e+00	0.2165

TABLE 5.3
Rough quadrilateral grids, reference space derived MPFA.

$1/h$	$\|p_h - p(\boldsymbol{x}_c)\|$	Rate	$\|\boldsymbol{u} - \Pi_h \boldsymbol{u}_h\|_h$	Rate	$\|\boldsymbol{u} - \boldsymbol{u}_h\|_h$	Rate
8	1.0757e-01	-	1.8941e+00	-	1.1895e+01	-
16	2.4504e-02	2.1342	5.8930e-01	1.6844	5.6694e+00	1.0691
32	5.9743e-03	2.0362	1.8020e-01	1.7094	2.7776e+00	1.0294
64	1.4998e-03	1.9940	6.2980e-02	1.5166	1.3736e+00	1.0159
128	3.8210e-04	1.9728	2.7009e-02	1.2215	6.8285e-01	1.0083
256	1.0820e-04	1.8203	1.2933e-02	1.0623	3.4062e-01	1.0034

TABLE 5.4
Rough quadrilateral grids, physical space derived MPFA.

6. Conclusions. This paper present a mixed finite element method with broken Raviart-Thomas elements and a specific quadrature rule. The effect is a block diagonal mass matrix, which can be inverted locally to find a discrete explicit flux for each half edge. Optimal first order convergence on rough grids is established for the Darcy velocity in a reduced $H(\mathrm{div})$ norm and for the pressure in the $\mathcal{L}_2$ norm. Compared to the reference space based MPFA method analyzed in [17], we gain better approximation on rough grids, but loose symmetry. In the Appendix the proposed mixed finite element method is shown to be equivalent to the physical space derived MPFA method proposed in [2].

REFERENCES

[1] I. Aavatsmark, *An introduction to multipoint flux approximations for quadrilateral grids*, Comput. Geosci., 6 (2002), pp. 404–432.

[2] I. Aavatsmark, T. Barkve, Ø. Bøe, and T. Mannseth, *Discretization on unstructured grids for inhomogeneous, anisotropic media. part i: Derivation of the methods. part ii: Discussion and numerical results*, SIAM J. Sci. Comput, 19 (1998), pp. 1700–1736.

[3] I. Aavatsmark, G. T. Eigestad, and R. A. Klausen, *Numerical convergence of MPFA for general quadrilateral grids in two and three dimensions*, IMA Volumes in Mathematics and its Applications, 142, Compatible spatial discretizations for partial differential quations (2006), pp. 1–22.

[4] I. Aavatsmark, G. T. Eigestad, R. A. Klausen, M. F. Wheeler, and I. Yotov, *Convergence of a symmetric MPFA method on quadrilateral grids*, Preprints, (2005).

[5] A. Agouzal, J. Baranger, J.-F. Maitre, and F. Oudin, *Connection between finite volume and mixed finite element methods for a diffusion problem with nonconstants coefficients. application to a convection diffusion problem*, East-West J. Numer. Math., 3 (1995), pp. 237–254.

[6] D. N. Arnold, D. Boffi, and R. S. Falk, *Approximation by quadrilateral finite elements*, Math. of Comp., 71 (2002), pp. 909–922.

[7] ———, *Quadrilateral H(div) finite elements*, SIAM J. Numer. Anal., 42 (2005), pp. 2429–2451.

[8] D. N. Arnold, D. Boffi, R. S. Falk, and L. Gastaldi, *Approximation by quadrilateral finite elements*, Comm. in Num. Meth. in Eng., 17 (2001), pp. 805–812.

[9] M. Berndt, K. Lipnikov, J. D. Moulton, and M. Shashkov, *Convergence of mimetic finite difference discretizations of the diffusion equation*, East-West J. Numer. Math., 9 (2001), pp. 130–148.

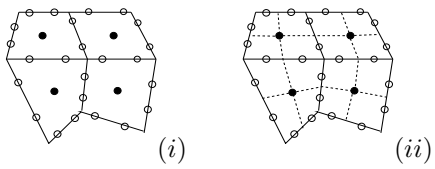

FIG. A.1. *(i). The degree of freedom associated with the MPFA method. The cell centered filled dots denote the cell pressure. The open dots denote the flux, and is calculated for each half cell edge. (ii). The subcells and dual grids by doted lines.*

[10] F. BREZZI AND M. FORTIN, *Mixed and hybrid finite element methods*, Springer, New York, 1991.

[11] S. CHOU, D. Y. KWAK, AND K. Y. KIM, *A general framework for constructing and analyzing mixed finite volume methods on quadrilateral grids: The overlapping covolume case*, SIAM J. Numer. Anal., 39 (2001), pp. 1170–1196.

[12] P. G. CIARLET, *The Finite Element Method for Elliptic Problems*, Noth-Holland Publishing Company, 1997.

[13] M. G. EDWARDS, *Unstructured, control-volume distributed, full-tensor finite-volume schemes with flow based grids*, Comput. Geosci., 6 (2002), pp. 433–452.

[14] G. T. EIGESTAD AND R. A. KLAUSEN, *On the convergence of the multi-point flux approximation o-method; numerical experiments for discontinous permeability*, Numer. Methods Partial Diff. Eqns, 21 (2005), pp. 1079–1098.

[15] R. A. KLAUSEN, *PhD thesis: On Locally Conservative Numerical Methods for Elliptic Problems; Application to Reservoir Simulation*, Dissertation, No 297, Unipub AS, Univ. of Oslo, 2003.

[16] R. A. KLAUSEN AND T. F. RUSSELL, *Relationships among some locally conservative discretization methods which handle discontinuous coefficients*, Comput. Geosci, 8 (2004), pp. 341–377.

[17] R. A. KLAUSEN AND R. WINTHER, *Convergence of multi point flux approximations on quadrilateral grids*, Preprint. Dept. of Math. Univ. of Oslo, Pure Maths. No. 3, (February 2005). To appear.

[18] J. WANG AND T. MATHEW, *Mixed finite element methods over quadrilaterals*, Proceedings of the 3th International Conference on Advances in Numerical Methods and Applications, Eds: I. T. Dimov, Bl. Sendov, and P. Vassilevskith., (1994), pp. 203–214.

[19] M. F. WHEELER AND I. YOTOV, *A cell-centered finite difference method on quadrilaterals*, IMA Volumes in Mathematics and its Applications, 142, Compatible spatial discretizations for partial differential quations (2006), pp. 189–208.

Appendix A. The Multi Point Flux Approximation.

The MPFA discretization is a control volume method, where more than two pressure values are used to find an explicit discrete flux expression. The unknowns are the cell pressures, and the half edge fluxes, cf. Figure A.1 (i). This appendix shows the derivation of MPFA from [2] in a mixed form and the equivalence to the perturbed non symmetric mixed finite element method (3.18). The derivation is preformed on quadrilateral grids where each interior vertex meets four cells. If the mapping F (2.1) is applied to the subcells instead of the global cell, the derivation easily generalize to both general quadrilaterals and triangles, with general cell center and edge continuity points.

Define a dual grid, $\mathcal{I}_h$, where the dual cells, denoted interaction regions $I \in \mathcal{I}_h$, consisting of the 4 subcells with a common vertex, cf. Figure A.1 (ii). Furthermore let $\mathcal{E}_h^{1/2}$ be the set of all the half edges created by dividing of the edges of $\mathcal{E}_h$ into two equal parts. Denote the subcells of I for E_j and the inner subcell edges for e_j, $j = 1, \ldots, 4$.

Define the pressure space $P(I)$ on the interaction region I to be all linear on the subcells E_j, which are continuous on the boundary of I. It is possible to chose other continuity points for each half edge. For each $p \in P(I)$ let $\{p_k\}_{k=1,\ldots,4}$ be the values of p at the corners of I, and $\{\lambda_k\}_{k=1,\ldots,4}$ the values of p at the continuity points, here

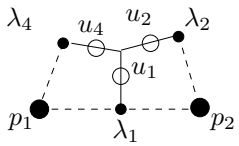

FIG. A.2. *On triangular or quadrilateral grids, the subcells are quadrilaterals. We let* $\bullet$ *denote the cell pressures* $\{p_1\}$*, the small* $\bullet$ *the cell edge pressure* $\{\lambda_1\}$*, and* $\circ$ *the edge velocities* $\{u_1\}$ *or edge flux.*

the edge midpoints, cf. A.2. The local pressure p is then uniquely defined by the 8 degrees of freedom $\{p_k, \lambda_k\}$. As before, let $\boldsymbol{K}_h$ be cellwise constant approximation of $\boldsymbol{K}$. Along half edge e of subcell E_j let

$$u_e|_{E_j} = -\boldsymbol{K}_h \operatorname{grad} p|_{E_j} \cdot \boldsymbol{n}_e. \tag{A.1}$$

The MPFA pressure space, $P_{\mathrm{MPFA}}(I)$, is now further restricted to

$$P_{\mathrm{MPFA}}(I) = \{p \in P(I) : [u_e]_e = 0,\ \forall e \in \mathcal{E}^{1/2}(I)\},$$

where $\mathcal{E}^{1/2}(I)$ represents the four inner edges of I, $[\,\cdot\,]_e$ is the jump across half edge e, and u_e is defined by (A.1).

LEMMA A.1. *The pressure* $p \in P_{\mathrm{MPFA}}(I)$ *is uniquely determined by the cell pressures* $\{p_k\}_{k=1,\ldots,4}$*, under the condition* (3.19).
The proof can be found in the end of this section.

In a control volume formulation, the discretization is down to approximate the flux. This can now be characterized locally on each interaction region. The normal-component associated a cell E can be defined from the mapping F. cf. (2.1) such that

$$[\boldsymbol{n}_1(\hat{x}), \boldsymbol{n}_2(\hat{y})] = \begin{bmatrix} y_{\hat{y}} & -y_{\hat{x}} \\ -x_{\hat{y}} & x_{\hat{x}} \end{bmatrix} = J\boldsymbol{D}^{-T}.$$

The subcell normals which are not cell normals is found for $\hat{y} = 1/2$ and $\hat{x} = 1/2$, and the cell normals is found for $\hat{y} = 0, 1$ and $\hat{x} = 0, 1$.

Consider the two subcells E_1 and E_2 with node pressure p_1 and p_2, and their common half edge e_1, see Figure A.2. Calculating the flux for half edge e_1 on subcell E_1 gives

$$u_1 = -\boldsymbol{K}_1 \operatorname{grad}(p)|_{E_1} \cdot \boldsymbol{n}_1(1)/2,$$

and similarly

$$u_4 = -\boldsymbol{K}_1 \operatorname{grad}(p)|_{E_1} \cdot \boldsymbol{n}_2(1)/2.$$

The linear variation in each subcell is spanned out by $\{\boldsymbol{n}_1(1/2), \boldsymbol{n}_2(1/2)\}$, such that the constant

$$\operatorname{grad}(p)|_{E_1} = \frac{1}{|\boldsymbol{n}_1(1/2) \times \boldsymbol{n}_2(1/2)|/2} [\boldsymbol{n}_1(1/2), \boldsymbol{n}_2(1/2)] \begin{pmatrix} p_1 - \lambda_1 \\ p_1 - \lambda_4 \end{pmatrix}.$$

Now $|\boldsymbol{n}_1(1/2) \times \boldsymbol{n}_2(1/2)| = J(1/2, 1/2)$. Summing up we have

$$\begin{aligned} \begin{pmatrix} u_1 \\ u_4 \end{pmatrix} &= -\frac{1}{J(1/2,1/2)} [\boldsymbol{n}_1(1), \boldsymbol{n}_2(1)]^T \boldsymbol{K} [\boldsymbol{n}_1(1/2), \boldsymbol{n}_2(1/2)] \begin{pmatrix} \lambda_1 - p_1 \\ \lambda_4 - p_1 \end{pmatrix} \\ &= \Lambda_{E_1}^{-1} \begin{pmatrix} p_1 - \lambda_1 \\ p_1 - \lambda_4 \end{pmatrix} \end{aligned}$$

Let the subscript c denote the reference cell center; $\hat{\boldsymbol{x}}_c = (1/2, 1/2)$, and the subscript i denote evaluation in cell vertices $\hat{\boldsymbol{x}}_i = (1,1), (0,1), (1,1)$ or $(0,1)$, for $i = 1, \ldots, 4$. Then on subcell E_i

$$\Lambda_{E_i}^{-1} = \frac{1}{J(\hat{\boldsymbol{x}}_c)} (J\boldsymbol{D}^{-T})^T(\hat{\boldsymbol{x}}_i)\boldsymbol{K}(J\boldsymbol{D}^{-T})(\hat{\boldsymbol{x}}_c)$$

which is invertible, and

$$\Lambda_{E_i} = \frac{1}{J(\hat{\boldsymbol{x}}_i)} \boldsymbol{D}^T(\hat{\boldsymbol{x}}_c)\boldsymbol{K}^{-1}\boldsymbol{D}(\hat{\boldsymbol{x}}_i). \tag{A.2}$$

Note that (A.2) is equivalent to the definition in (3.11). For subcell E_1 and E_2, cf. Figure A.2, we now have

$$\Lambda_{E_1} \begin{pmatrix} u_1 \\ u_4 \end{pmatrix} = \begin{pmatrix} p_1 - \lambda_1 \\ p_1 - \lambda_4 \end{pmatrix} \qquad \text{and} \qquad \Lambda_{E_2} \begin{pmatrix} u_1 \\ u_2 \end{pmatrix} = \begin{pmatrix} \lambda_1 - p_2 \\ p_2 - \lambda_2 \end{pmatrix}. \tag{A.3}$$

Eliminating λ_1, and let the components of Λ_{E_j} be denoted κ_{kl}^j, for $k, l = 1, 2$, result in the equation

$$(\kappa_{11}^1 + \kappa_{11}^2)u_1 + \kappa_{12}^1 u_4 + \kappa_{12}^2 u_2 = -(p_2 - p_1) \tag{A.4}$$

associated the edge e_j. By deriving the similar equations for the other interior edges of I we obtain a 4×4 system of the form

$$\boldsymbol{A}\boldsymbol{u} = \boldsymbol{b}, \tag{A.5}$$

where the components of $\boldsymbol{b}$ are pressure difference, $\boldsymbol{u} = (u_1, \ldots, u_4)^T$, and

$$\boldsymbol{A} = \begin{pmatrix} (\kappa_{11}^1 + \kappa_{11}^2) & \kappa_{12}^2 & 0 & \kappa_{12}^1 \\ \kappa_{21}^2 & (\kappa_{22}^2 + \kappa_{22}^3) & \kappa_{21}^3 & 0 \\ 0 & \kappa_{12}^3 & (\kappa_{11}^3 + \kappa_{11}^4) & \kappa_{12}^4 \\ \kappa_{21}^1 & 0 & \kappa_{21}^4 & (\kappa_{22}^4 + \kappa_{22}^1) \end{pmatrix}. \tag{A.6}$$

Note that A is not symmetric, unless the involved cells are parallelograms. To ensure stability we will have to impose the stability criteria (3.19) on each subcell. This ensures the symmetric part of $\Lambda = (\Lambda + \Lambda^T)/2 + (\Lambda - \Lambda^T)/2$ to be positive definite.

Recall that the space $\mathcal{RT}_h^{1/2}$ has a canonical basis derived from the degrees of freedom on each half edge in $\mathcal{E}_h^{1/2}$. With the basis function associated half edge e_1, $v|_{e_k} = 1$ for $k = 1$ and 0 for $k \neq 1$, the left part of equation (A.4) also appears from (3.14). It is easy to see that the mass matrix corresponding to the canonical basis and the bilinear form a_h is block diagonal, where the 4×4 diagonal blocks correspond to the 4 half edges meeting vertices of $\mathcal{T}_h$, or equivalently, to each interaction region of $\mathcal{I}_h$. Hence, blocks resemble the structure of the matrix $\boldsymbol{A}$ given by (A.6). The second term of the first equation in (3.18) gives a pressure difference. Therefore, for each interaction region the first equation of (3.18) corresponds exactly to the system (A.5). Summing up, we have following result.

THEOREM A.2. *The perturbed non symmetric mixed finite element method* (3.18) *is equivalent to the physical space derived MPFA method.*

Finely, we show the proof of Lemma A.1.

Proof. Lemma A.1. It is enough to show that if $\hat{p} \in P_{\text{MPFA}}(I)$, with $\{p_k\}_{k=1,2,3,4}$ all equal zero, then $\{\lambda_k\}_{k=1,2,3,4}$, must also be zero. Under the assumption $p_k = 0$

it follows from (A.1) and (A.3) that the constraint of continuous flux leads to the system

$$\boldsymbol{A}'\boldsymbol{\lambda} = 0 \tag{A.7}$$

with $\boldsymbol{\lambda} = (\lambda_1, \lambda_2, \lambda_3, \lambda_4)^T$ and

$$\boldsymbol{A} = \begin{pmatrix} (\kappa_{11}^1 + \kappa_{11}^2) & -\kappa_{12}^2 & 0 & \kappa_{12}^1 \\ -\kappa_{21}^2 & (\kappa_{22}^2 + \kappa_{22}^3) & \kappa_{21}^3 & 0 \\ 0 & \kappa_{12}^3 & (\kappa_{11}^3 + \kappa_{11}^4) & -\kappa_{12}^4 \\ \kappa_{21}^1 & 0 & -\kappa_{21}^4 & (\kappa_{22}^4 + \kappa_{22}^1) \end{pmatrix}.$$

The symmetric part of this matrix consists of the sum of the symmetric parts of Λ_{E_j}, $j = 1, \ldots, 4$, and is therefore positive definite under condition (3.19). The minus signs do not alter this. Multiplying equation (A.7) by $\boldsymbol{\lambda}$, and it follows that $\boldsymbol{\lambda} = 0$. □